

APS TBC Performance on Directionally-Solidified Superalloy Substrates with HVOF
NiCoCrAlYHfSi Bond Coatings

M. J. Lance, K. A. Unocic, J. A. Haynes and B. A. Pint

Materials Science and Technology Division

Oak Ridge National Laboratory, 1 Bethel Valley Rd., Oak Ridge, TN 37831, USA

Directionally-solidified (DS) superalloy components with advanced thermal barrier coatings (TBC) to lower the metal operating temperature have potential to replace more expensive single crystal superalloys for large land-based turbines. In order to assess relative TBC performance, furnace cyclic testing was used with superalloys 1483, X4 and Hf-rich DS 247 substrates and high velocity oxygen fuel (HVOF)-NiCoCrAlYHfSi bond coatings at 1100 °C with 1-h cycles in air with 10% H₂O. With these coating and test conditions, there was no statistically-significant effect of substrate alloy on the average lifetime of the air plasma sprayed (APS) yttria-stabilized zirconia (YSZ) top coatings on small coupons. Using photo-stimulated luminescence spectroscopy maps at regular cycling intervals, the residual compressive stress in the α -Al₂O₃ scale underneath the YSZ top coating and on a bare bond coating was similar for all three substrates and delaminations occurred at roughly the same rate and frequency. X-ray fluorescence (XRF) measurements collected from the bare bond coating surface revealed higher levels of Ti interdiffusion occurring on the 1483 substrate, which contained the highest Ti content.

Keywords: photo-stimulated luminescence piezospectroscopy (PLPS); water vapor; bond coating; alumina scale; TBC; directionally-solidified superalloy

1. Introduction

The U.S. Department of Energy's Advanced Turbine Systems Program (1994-2001), in conjunction with the turbine industry, helped to transfer the best aero-engine materials technology (i.e. thermal barrier coatings (TBC) and single crystal superalloys) leading to increases in the efficiency of land-based turbines [1, 2]. However, the long time (>25,000h), near-constant metal temperature operating conditions required for power generation appears to have resulted in a different materials paradigm than for aero-engines. Rather than being dominated by high metal temperatures at takeoff and landing, the lower constant temperatures may switch the primary driving force for TBC failure from a thermo-mechanical to a chemical mechanism, i.e. Al depletion of the bond coating due to interdiffusion [3].

Furthermore, the lower metal operating temperatures do not require the highest performance superalloys, thereby allowing engine manufacturers to use lower cost superalloys for the much larger land-based turbine components. Less expensive superalloys may be single crystals without Re, such as first generation alloys like 1483 or Re-free second generation alloys like N500 or X7 [4-6] or further dropping to directionally solidified superalloys. The current study builds upon prior work [7-9] studying the performance of NiCoCrAlYHfSi [10] bond coatings deposited by HVOF and examines how changes in the superalloy substrate affects the TBC lifetime in furnace cycle testing. Surprisingly, the coating lifetime was not affected by the substrate composition. Measurements of the residual stress beneath the APS YSZ top coating at regular cycling intervals [9] also revealed few differences.

2. Material and methods

A commercial NiCoCrAlYHfSi powder (PWA286) was used to coat superalloy coupons, 1.69 cm in diameter, of X4, 1483 and 247 using a commercial-type HVOF process at Stony

Brook University's Center for Thermal Spray Research. The measured compositions of the superalloys and the bond coating powder are listed in Table I. The coated specimens were annealed for 4h at 1080 °C and had a bond coating thickness of ~160 μm. A 200 μm thick multi-layer of APS YSZ top coat [11] was applied to one side of the specimen. Four specimens of each coated substrate were furnace cycled at 1100 °C in 1-h cycles in 10±1 vol.% H₂O; three with YSZ and one with only a bond coating. One set of four specimens on 247 was exposed to dry air for comparison.

As described in detail elsewhere [8, 9, 12], samples were periodically examined with a Keyence VHX digital microscope and a Dilor XY800 Raman microprobe (Horiba Scientific, Edison, NJ) to map the change in surface height and residual stress in the Al₂O₃ scale, respectively. The same region was mapped following subsequent heat treatments which allowed stress evolution at the YSZ-bond coating interface to be monitored. In addition, microscopic x-ray fluorescence (μ-XRF) was also collected from one spot on the bare bond coating specimens in the same location as the PLPS maps using a Shimadzu μEDX 1300 spectrometer. Chemical composition was estimated using the fundamental parameters method assuming a homogenous substrate. This will be discussed in more detail below. After failure, the specimens were metallographically sectioned, polished and examined by light microscopy and electron probe microanalysis (EPMA) using a JEOL model 8200 microprobe.

3. Results and discussion

Fig. 1 shows the average TBC lifetime on the three different substrates in 10% H₂O and in dry air for the 247 substrate following 1 h cycles at 1100 °C. The superalloy substrate had no effect on the TBC lifetimes. This suggests that the lower cost 247 alloy may provide the same level of coating durability as more advanced superalloy compositions. There was also no

difference in TBC lifetime between specimens cycled in 10% H₂O and dry air on the 247 substrate. This is the opposite of previously reported results [9] on 1483 and X4 which found a decline in TBC lifetime from dry air to water vapor environments for 1 h cycles at 1100 °C. In order to better understand this difference, TBC lifetimes of a previous batch [9] of specimens (batch 2) with a thinner bond coating (~90 μm) on X4 and 1483 are also included in Fig. 1. Bar charts of the bond coating thicknesses are shown in Fig. 2. The 1483 substrate had a shorter TBC lifetime than the X4 substrate for batch 2) which was attributed to lower Al content in the 1483 bond coating caused by higher rates of interdiffusion. The thicker bond coating in the current batch (batch 3) of specimens may be slowing onset of detrimental interdiffusion effects, thereby eliminating any substrate effect on TBC lifetime at this temperature. The thicker bond coating may also reduce the negative impact of water vapor on TBC lifetime observed on the 247 substrate. The average roughness (R_a) of the bond coats in this study was ~8 μm, which was the same as the previous thinner bond coating [9].

Fig. 3 shows stress maps following 1 h and 200 h at 1100 °C for all three substrates in air with 10% H₂O and 247 in dry air. The bare bond coating specimen on 247 is also included. On the YSZ coated samples the same trend is observed: 1.0 to 1.5 GPa of compressive stress in most locations with a few locations at near-zero stress. These near-zero stress regions increase in frequency following cycling indicating that localized alumina scale cracking is occurring at the interface with cycling. The size and frequency of the near-zero stress regions correspond to large spherical particles that were produced by over spraying with coarser powder in order to increase the bond coating roughness [9]. During thermal cycling, these particles will generate out-of-plane tensile stresses [13] that may lead to scale cracking producing the near-zero stress regions in Fig. 3. Subsequent cycling will cause these cracked regions to grow in frequency and size eventually resulting in YSZ delamination. In contrast, the scale grown on the bare bond coating on 247

showed a much larger stress distribution indicating that the scale delaminates much more readily compared to when a TBC is present. Thus, the presence of the YSZ appears to support the stability and adhesion of the underlying alumina layer.

Fig. 4 shows the data from Fig. 3 represented as box plots for all heating durations. The YSZ-coated specimens decrease in stress with thermal cycling due to the growth of the near-zero stress regions. The stress in the scale of the bare bond coating specimen has a larger distribution throughout the duration of the test. Starting at 100 cycles, the stress on the bare bond coating specimen increases due to the formation of fresh intact scale on regions where the scale has spalled.

Fig. 5 compares the stress histograms of the bare bond coating and the YSZ coated specimens on 247. Again, the YSZ coated sample has a much narrower stress distribution due to the constraint imposed by the TBC on the Al_2O_3 scale. The large difference between the stress profiles of these two samples indicates that stress measurements on the bare bond coating is of limited value for understanding stress generation and delamination in YSZ coated samples.

Fig. 6 shows the EPMA line profile for a YSZ-coated specimen with a 247 substrate and a bond coating thickness of 180 μm after exposure to 480 1 h cycles at 1100 $^\circ\text{C}$ in air with 10% H_2O . The Al content has dropped to ~6 wt. % which is the Al content of the 247 alloy and is far below the starting composition of the bond coating at 12.3 wt. %. Further reduction in the Al content adjacent to the scale will eventually be deleterious to alumina scale adhesion, although the Al content of the coating has equilibrated with the substrate and the critical Al depletion level for this system has not been identified.

While being useful for understanding interdiffusion, EPMA is a destructive technique that can only be performed following metallography. XRF, which also measures the characteristic x-rays emitted by elements following ionization, however induced with x-rays instead of electrons,

is non-destructive and, unlike electron-based techniques, penetrates deep enough into the surface to probe the bond coating composition through the oxide scale on a bare bond coat. The penetration depth (t) is determined by the density of the material (ρ) and the weight-averaged mass attenuation coefficients (μ/ρ) [14] through the equation:

$$t = -\frac{\ln\left(\frac{I}{I_0}\right)}{\left(\frac{\mu}{\rho}\right)*\rho} \quad [1]$$

Using a value 0.05 for the ratio I/I_0 assumes all but 5% of the x-rays have been attenuated by the material and gives a penetration depth into the bond coating of $\sim 25 \mu\text{m}$ for x-rays with energies between 5 and 10 keV such as those from W and Ti. Figs. 7a and b show the concentration of W and Ti, respectively, measured non-destructively with XRF on the surface of the bare bond coating with a penetration depth of $25 \mu\text{m}$. Also included Fig. 7 are the average concentrations of these elements measured within the first $25 \mu\text{m}$ of the bond coating surface using EPMA cross-sectional profiles on YSZ coated samples all of which failed at 480 h from Fig. 6. Figure 7a shows an increase in the W concentration following cycling at $1100 \text{ }^\circ\text{C}$ for all three substrates with the largest increase with the 247 alloy which also had the highest W concentration of the three alloys (10.0 wt. %). The W concentration measured with EPMA is more than twice that measured with XRF for 247 but is the same for 1483. Titanium shows a much better correspondence between XRF and EPMA measurements with the 1483 alloy having the highest concentration. This is expected due to the higher Ti concentration in the 1483 alloy (4 wt. %) versus 1 wt. % for 247 and X4.

XRF greatly overestimates the concentration of Al when compared to EPMA results (Fig. 7c). This is due to the fact that the Al $K\alpha$ x-rays emit at 1.486 keV, much lower than W (8.396 keV) and Ti (4.51 keV) which greatly reduces the depth penetration for Al. Using Eq. 1, the penetration depth for detecting Al through the bond coating is estimated to be $\sim 1 \mu\text{m}$, so the

signal comes almost entirely from the Al_2O_3 scale, hence the high Al composition measured by XRF in Fig. 7c. This shows that XRF is a useful nondestructive technique that can track changes in heavier elements in a near surface zone, but is not useful for determining Al depletion.

Backscattered electron images of TBC cross sections from the batch 2 and batch 3 on the X4 substrate after TBC failure are shown in Fig. 8(a) and (b), respectively. Other than the much thicker bond coating in the current batch, there were no microstructural differences between the two batches. Additionally, no significant microstructural differences were observed between the three alloys in this study or between the TBC-coated 247 alloy heated in 10% H_2O and the sample heated in air.

4. Conclusion

Three different superalloy substrates (X4, 1483 and 247) with the same thermally sprayed TBC coating were evaluated in 1-h cycles at 1100 °C in air with 10% H_2O . Under these conditions, no statistically-significant effect of the substrate on the average TBC lifetime was observed with the relatively thick ($>150\mu\text{m}$) HVOF NiCoCrAlYHfSi bond coating and a multilayer YSZ top coating. The residual stress in the thermally grown alumina scale beneath the YSZ top coating was mapped in a fixed region at regular cyclic intervals and also did not show any effect of the superalloy substrate, consistent with the lifetime observations. Also, x-ray fluorescence spectroscopy was used to non-destructively track the near-surface composition of bare bond coating specimens of each superalloy substrate. While this technique cannot determine the remaining Al content in the coating, it was able to measure heavier elements such as Ti, which was highest in the coating on the 1483 substrate with the highest Ti content in the alloy.

Acknowledgements

The authors would like to thank D. Leonard, G. Garner, T. Lowe, T. Geer and T. Jordan for assistance with the experimental work at ORNL and E. Lara-Curzio and P. F. Tortorelli for comments on the manuscript. This research was sponsored by the U.S. Department of Energy, Office of Coal and Power R&D in the Office of Fossil Energy, (R. Dennis program manager).

References

- [1] W.P. Parks, E.E. Hoffman, W.Y. Lee, I.G. Wright, *J. Thermal Spray Technol.*, 6 (1997) 187-192.
- [2] P.A. Hoffman, *MRS Bull.*, 23 (1998) 4-7.
- [3] H. Echsler, D. Renusch, M. Schutze, *Mater. Sci. Tech.*, 20 (2004) 307-318.
- [4] P.J. Fink, J.L. Miller, D.G. Konitzer, *JOM*, 62 (2010) 55-57.
- [5] J.B. Wahl, K. Harris, *Superalloys 2012*, (2012) 179-188.
- [6] B.A. Pint, *Mater. Sci. Tech.*, 30 (2014) 1387-1391.
- [7] J.A. Haynes, K.A. Unocic, B.A. Pint, *Surf. Coat. Tech.*, 215 (2013) 39-45.
- [8] J.A. Haynes, K.A. Unocic, M.J. Lance, B.A. Pint, *Surf. Coat. Tech.*, 237 (2013) 65-70.
- [9] M.J. Lance, K.A. Unocic, J.A. Haynes, B.A. Pint, *Surf. Coat. Tech.*, 260 (2014) 107-112.
- [10] J.T. Demasi-Marcin, D.K. Gupta, *Surf. Coat. Tech.*, 68 (1994) 1-9.
- [11] V. Viswanathan, G. Dwivedi, S. Sampath, *J. Amer. Cer. Soc.*, 97 (2014) 2770-2778.
- [12] M.J. Lance, K.A. Unocic, J.A. Haynes, B.A. Pint, *Surf. Coat. Tech.*, 237 (2013) 2-7.
- [13] C.H. Hsueh, J.A. Haynes, M.J. Lance, P.F. Becher, M.K. Ferber, E.R. Fuller, S.A. Langer, W.C. Carter, W.R. Cannon, *J. Amer. Cer. Soc.*, 82 (1999) 1073-1075.
- [14] NIST X-Ray Mass Attenuation Coefficients, in, <http://www.nist.gov/pml/data/xraycoef/index.cfm>.

Table I. Chemical compositions (weight % or ppmw) determined by inductively coupled plasma analysis and combustion analysis.

Material	Ni	Cr	Al	Re	Co	W	Ta	Mo	Ti	C	Other (ppmw)
X4	60.8	6.4	5.8	2.9	9.5	6.4	6.5	0.6	1.0	<	<3Y,800Hf,9S
1483	60.6	12.0	3.4	<	8.8	4.1	5.2	1.9	4.0	0.07	<3Y,20Hf,40Si,<1S
247	59.1	8.5	5.6	0.02	10.2	10.0	3.2	0.62	1.0	0.16	<3Y,13200Hf, 600Si, 11S
MCrAlYHf	48.0	16.7	12.3	<	21.6	0.01	<	<	<	0.01	6820Y,2500Hf, 3600Si,2S

< Indicates below the detectability limit of <0.01 wt. %.

List of figure captions

Figure 1. TBC lifetimes following 1 hour cycles at 1100 °C on three different substrates. The previous batch of samples were tested in air + 10% H₂O. The error bars are the standard deviation of 3 measurements.

Figure 2. Box plots showing bond coating thicknesses measured from cross-sectioned images of the three alloys (DS247, 1483 and X4) and from the previous (Batch 2) and current batch (Batch 3).

Figure 3. PLPS stress maps collected from the Al₂O₃ scale underneath the YSZ coating on the X4, 1483 and 247 substrates in air + 10% H₂O and on the 247 substrate in dry air. The Al₂O₃ stress map on the bare bond coating on 247 cycled in air + 10% H₂O is also included.

Figure 4. Box plots of the stress measurements for all cycling durations on all 5 samples shown in Fig. 3. The error bars are set at 1st and 99th percentile.

Figure 5. Stress histograms collected from the Al₂O₃ scale through a YSZ top coating (a) and on a bare bond coating (b) on the 247 alloy.

Figure 6. EPMA chemical composition measured on a cross section of a TBC coated 247 alloy after 480 h of cycling at 1100 °C in 10% H₂O.

Figure 7. μ -XRF compositional measurements collected on bare bond coating specimens cycled in 10% H₂O at 1100 °C for (a) W, (b) Ti and (c) Al. The EPMA compositions averaged across the top 25 μ m of the TBC coated samples are also included.

Figure 8. Backscattered electron images of the TBC-coated X4 substrate from batch 2 after 380 1 h cycles (a) and batch 3 after 480 1h cycles (b) in 10% H₂O at 1100 °C.

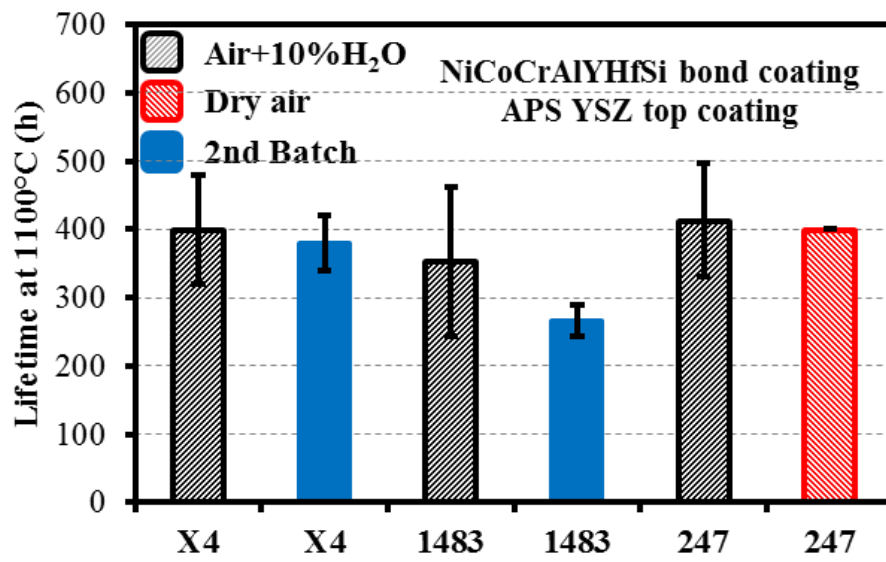


Fig. 1.

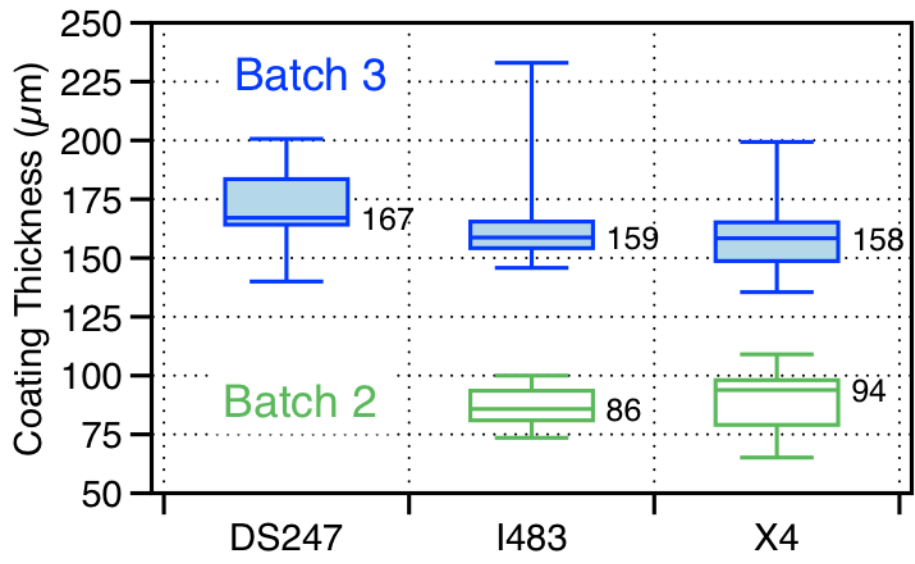


Fig. 2.

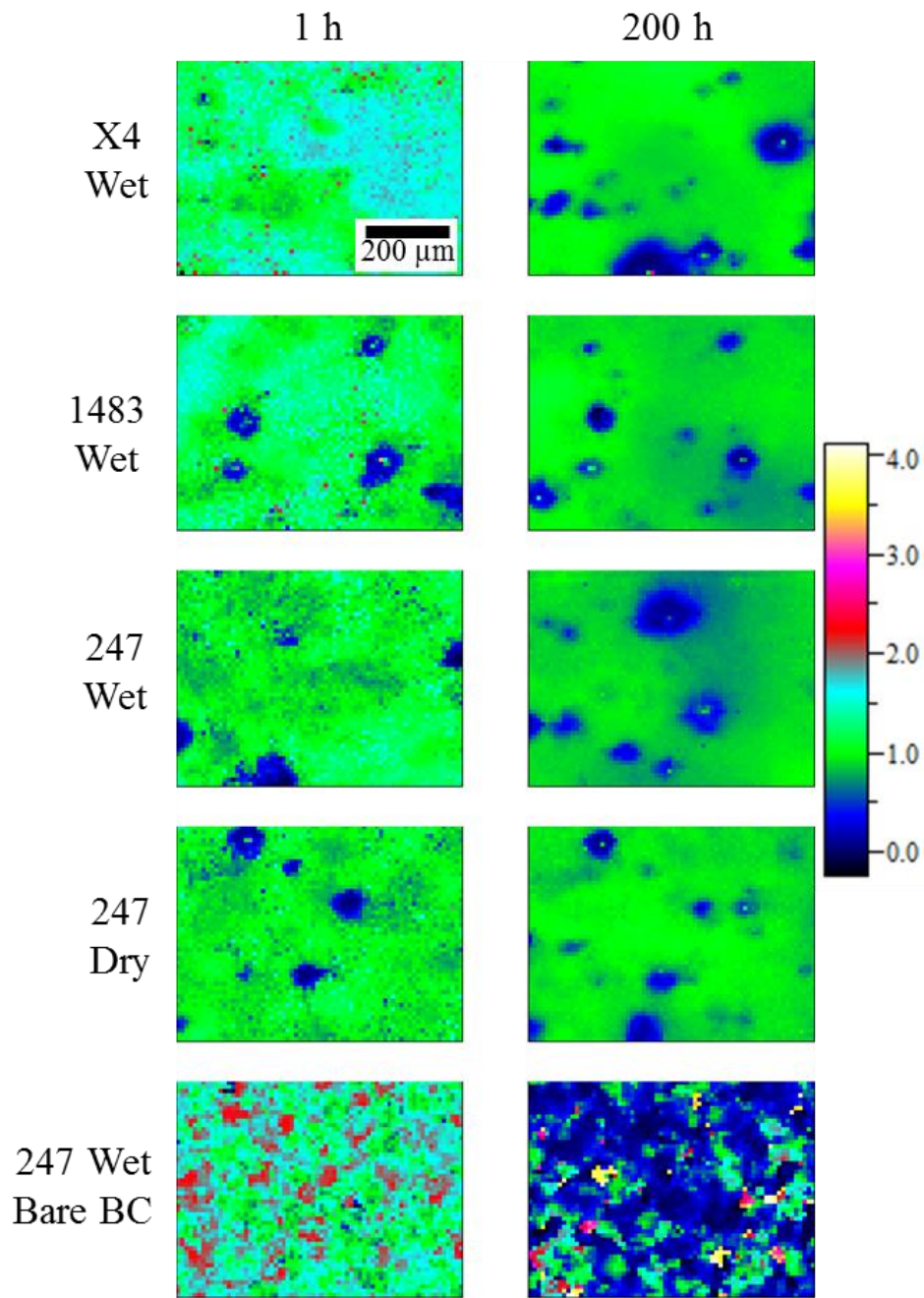


Fig. 3.

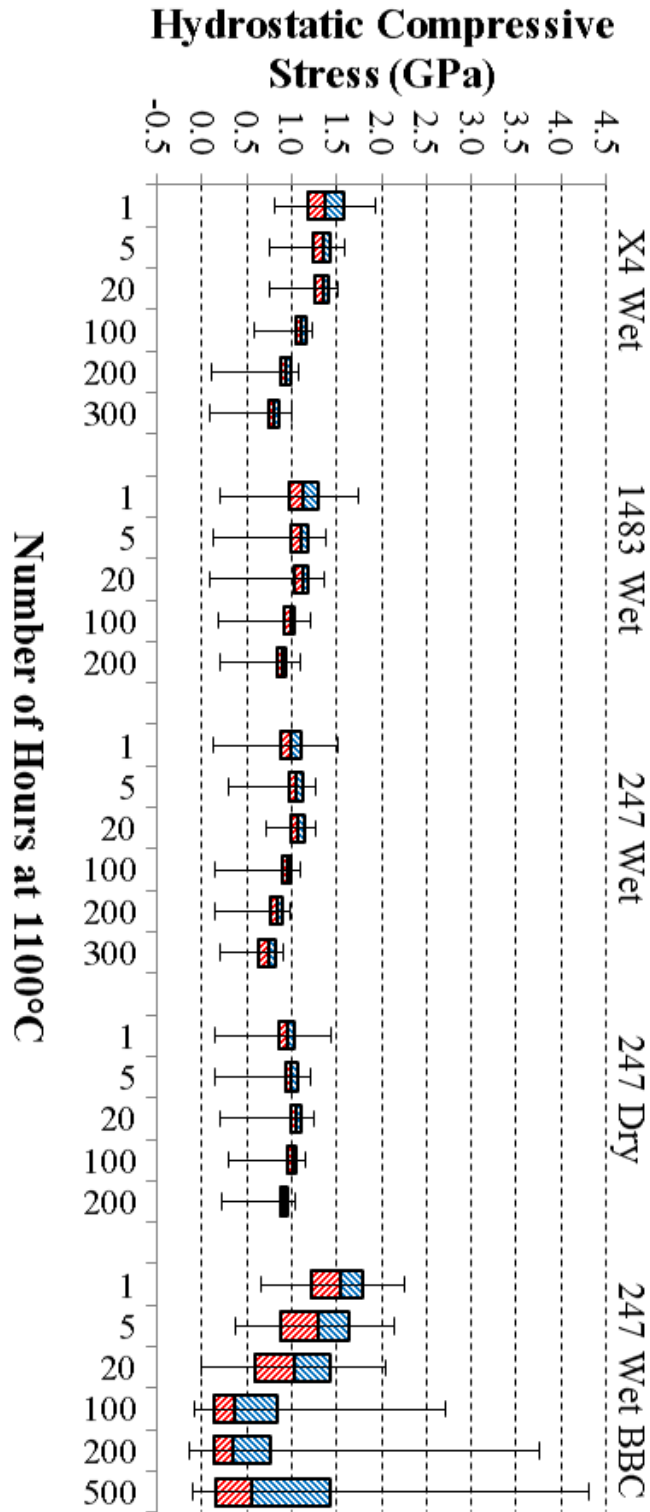


Fig. 4.

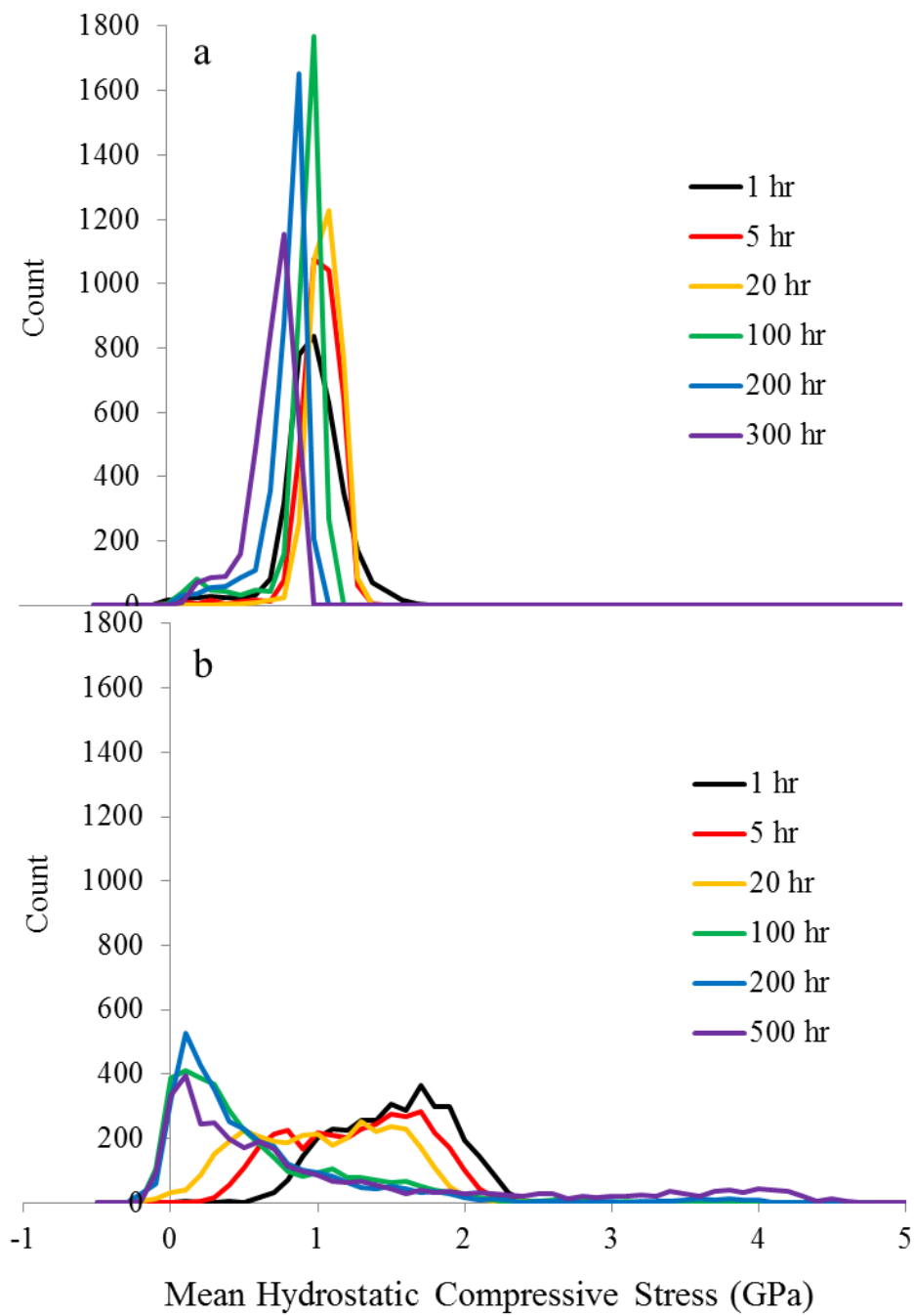


Fig. 5.

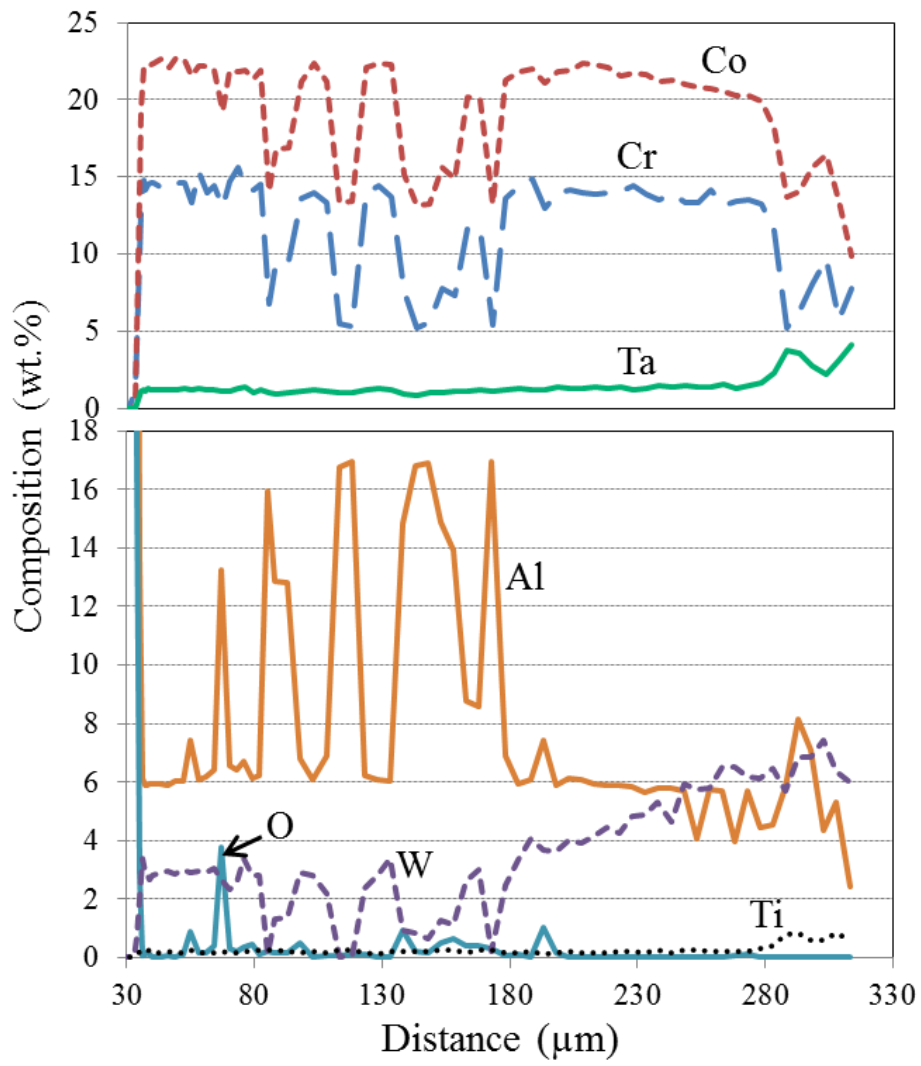


Fig. 6.

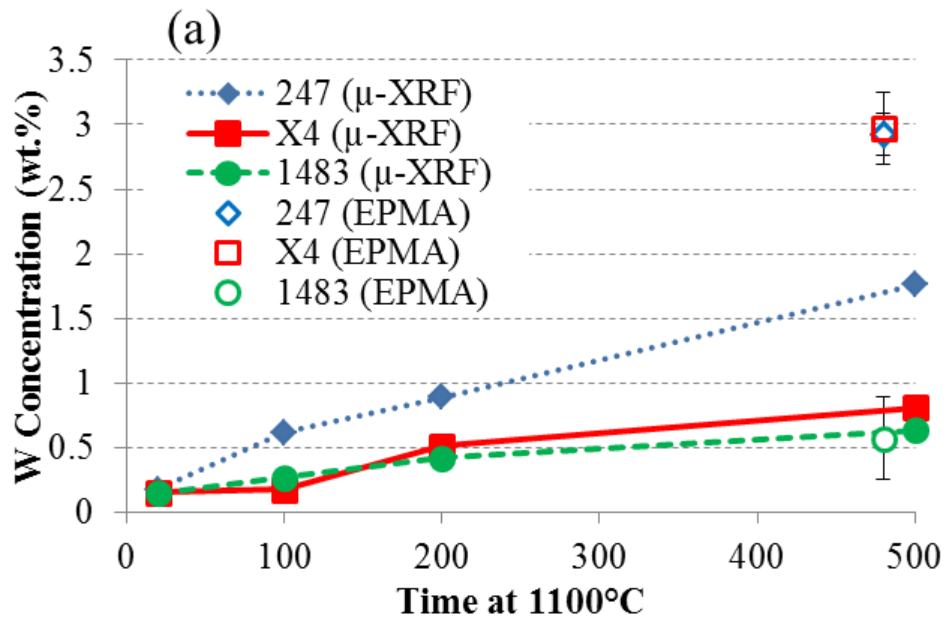


Fig. 7a.

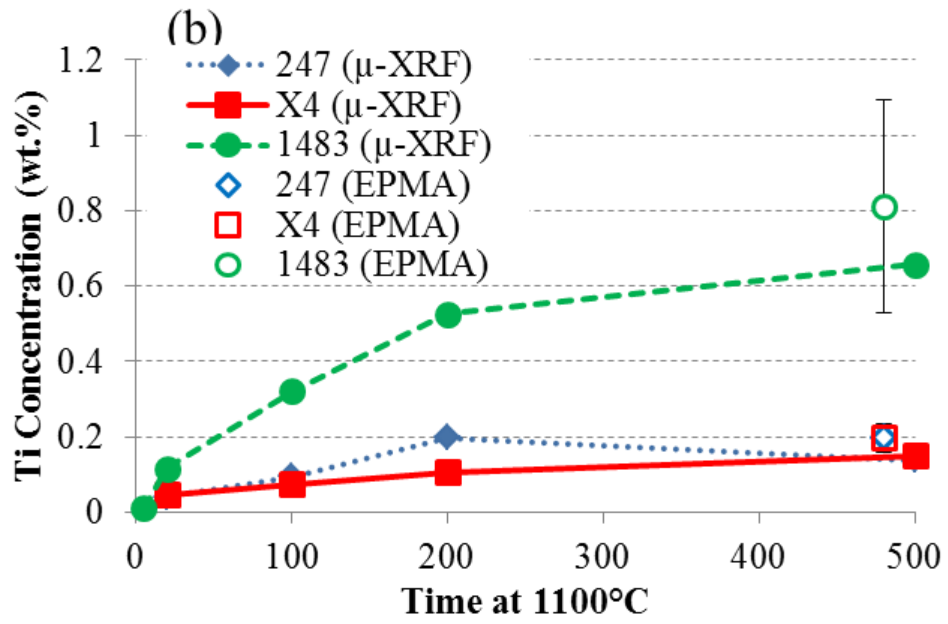


Fig. 7b.

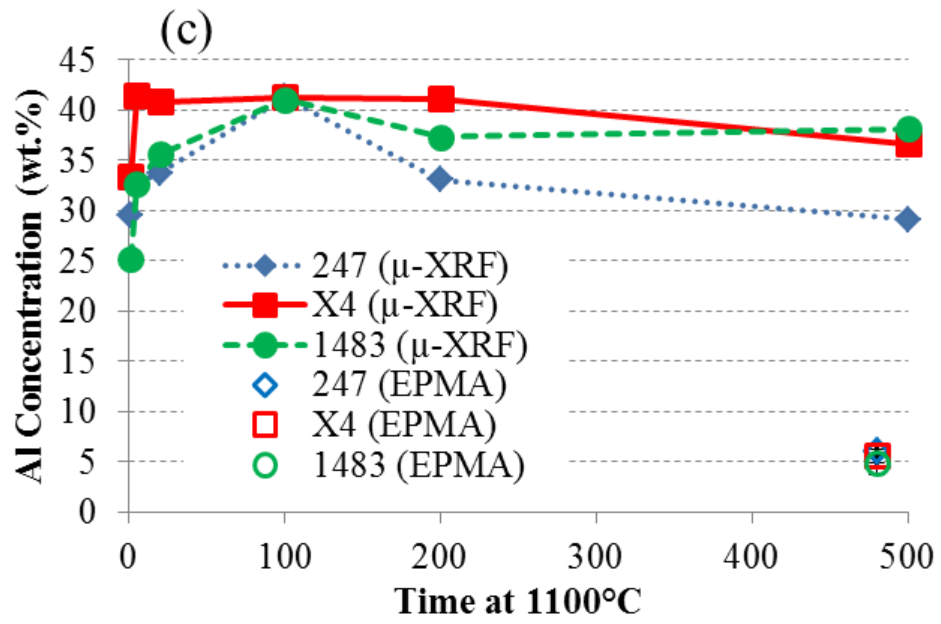


Fig. 7c.

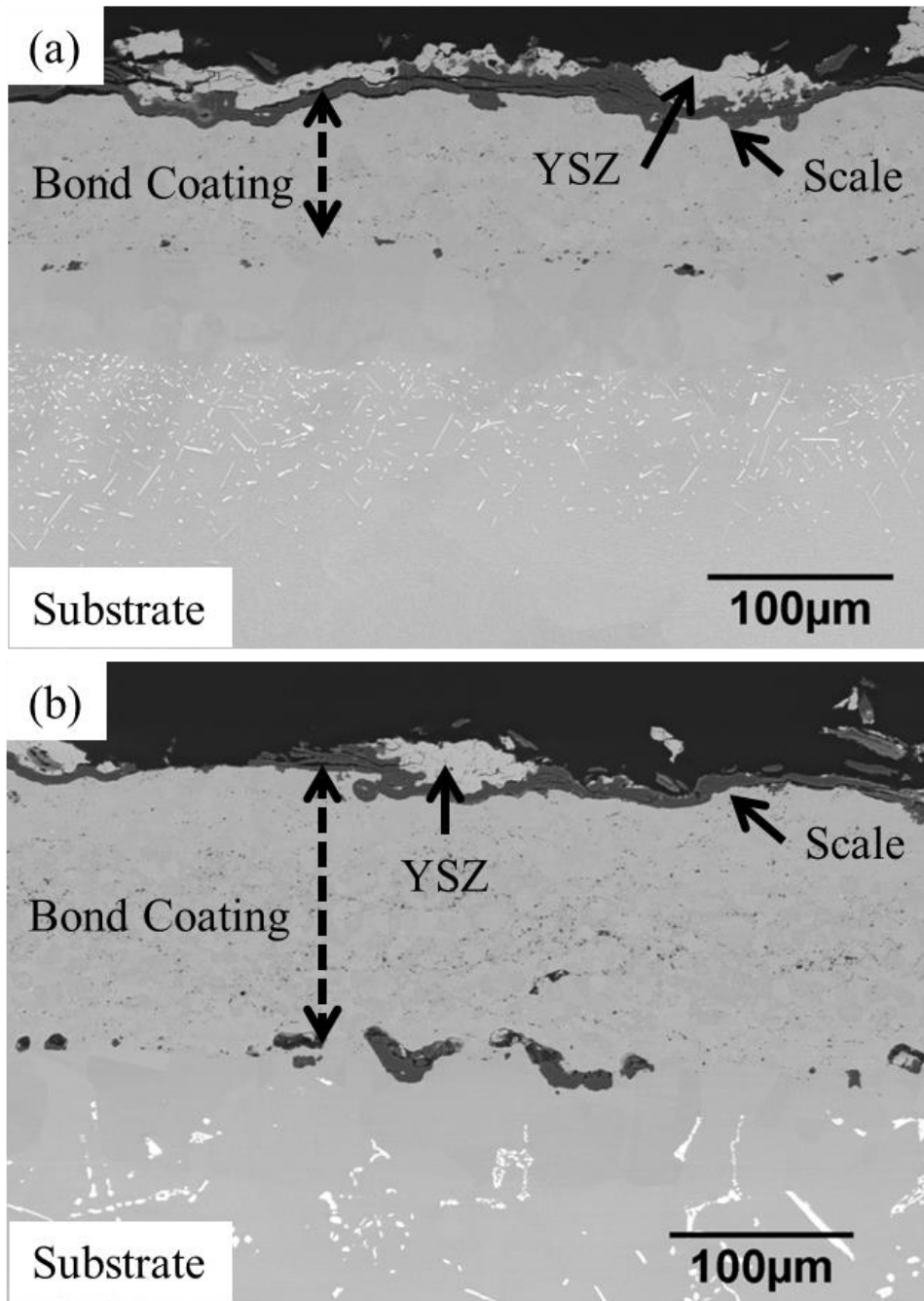


Fig. 8.